The simulation of a wave propagation in a bcc iron crystal with a crack

V. Pelikán[a,*], P. Hora[a], A. Machová[b], O. Červená[a]

[a] *Institute of Thermomechanics of the ASCR, v.v.i., Veleslavínova 11, 301 14 Plzeň, Czech Republic*
[b] *Institute of Thermomechanics of the ASCR, v.v.i., Dolejškova 5, 182 00 Praha, Czech Republic*

Received XX June XXXX; received in revised form YY July YYYY

Abstract

We present a large-scale molecular dynamic simulations of a wave propagation in a bcc iron based on a N-body potential model which gives a good description of an anisotropic elasticity. A crack is embedded in a bcc iron crystal having a basic cubic orientation. We consider a central pre-existing Griffith (through) crack. The crystal is loaded on its front face and the response is detected on its opposite face. The acquired results are very important for the new NDT nano scale methods.

Keywords: molecular dynamics, bcc iron crystal, wave propagation

1. Introduction

In this article we describe 3D simulations of elastic wave propagation in a bcc iron based on molecular dynamic (MD) method. A central Griffith (through) crack is embedded in a bcc iron crystal with the basic cubic orientation. This research is a continuation of the topics mentioned in [4] and [5]. There is described the behavior of stress waves caused by a surface impulsion in perfect crystals. In present simulations we use an N-body potential of a Finnis-Sinclair type for transition metals, [1] and [2]. We study mechanical response of the crack to the applied pressure stress waves in the framework of the non-linear atomistic model.

The tasks of this type have a physical sense only if the information is not influenced by the stress waves reflections from the free surfaces of atomistic samples. For that reason the samples should be large enough and the simulations on these models can be realized only with a massive application of parallel programming techniques, [3].

2. Description of numerical MD experiments

All MD simulations were performed on a bcc iron plates with the lattice constant $a_0 = 2,8665$ Å. The plate thickness was 400 atoms (sample A) or 200 atoms (sample B) in the y axis direction. The infinity in the other two directions was reached by the application of the periodic boundary conditions on the rectangular sample with the edge of 400 atoms in the x axis direction and the edge of 500 atoms in the z axis direction, see fig. 1. The thickness of the Griffith (through) crack corresponds 2 atoms and height 100 atoms in both samples, see fig. 1. The sample A contains totally 159 680 400 atoms, sample B 79 680 400 atoms. Surface relaxation

*Corresponding author. Tel.: +420 377 236 415, e-mail: pelikan@cdm.it.cas.cz.

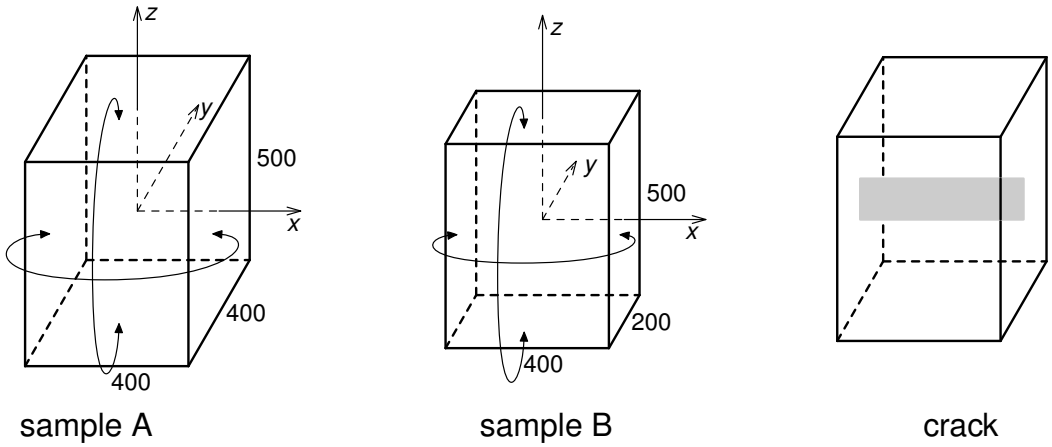

Fig. 1. The geometry of used samples and the crack location.

has been performed in the samples before external loading. Initial temperature corresponds to 0 K and further thermal atomic motion is not controlled in the system.

To solve Newtonian equations of motion we used time integration step 10^{-14} s in all the simulations. The tests were done between the steps 0 and 3000 for the sample A and between the steps 0 and 1500 for the sample B. The total energy balance (the kinetic energy, the potential energy and the work of external forces), the total number of the atomic interactions, and the local number of the atomic interactions at free crack faces were monitored at each time step. The total number of the interactions was either constant (1 116 320 400 for the sample A and 556 320 400 for the sample B) or increased by the number of the local through crack interactions, which do not exist initially across the free crack faces.

The applied external stress has been increased from zero to a maximum value during 30 time integration steps. We have been used ten various levels of the applied stress. In tab. 1, the values of applied stress are given both via Young's modulus ratio and in GPa.

Number of level	Applied stress	
	E [%]	[GPa]
1	1/4	0.3375
2	1/2	0.6750
3	1	1.3500
4	2	2.7000
5	4	5.4000
6	8	10.800
7	16	21.600
8	32	43.200
9	64	86.400
10	128	172.80

Tab. 1. The applied stress levels.

Three different classes of the loading were tested on the samples, see fig. 2:

1. all-area excitation in the y axis direction on the front side,
2. line excitation in the y axis direction in the middle of the front side, parallel to the x axis,
3. point excitation in the y axis direction in the middle of the front side.

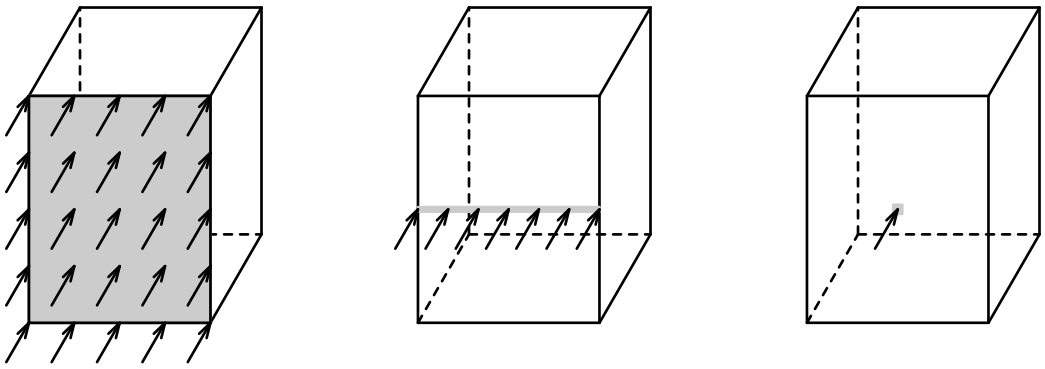

Fig. 2. The type of loading.

The calculations for the sample A were done on 50 CPUs cluster SKIRIT at the Masaryk University Brno (implementation of one simulation step corresponded in average 21 s). The calculations for the sample B were done on 30 CPUs cluster MINOS at the University of West Bohemia Pilsen (implementation of one simulation step corresponded in average 40 s).

3. Results and discussion

The simulations performed are marked in tab. 2 for individual levels of loading and the type of loading. The ^{p} marks denote the simulations, where a plastic deformation occurred after loading. The $*$ marks denote the simulations, where the local atomic interactions across the free crack faces were monitored.

	Sample A			Sample B		
	plane	line	point	plane	line	point
1	✓			✓		
2	✓*			✓*		
3	✓*	✓	✓	✓*		
4	✓*	✓	✓	✓*		
5	✓*	✓	✓	✓*		
6	✓*	✓	✓	✓*	✓	✓
7		✓	✓		✓	✓
8		✓^{p}	✓^{p}		✓^{p}	✓^{p}
9		✓^{p}	✓^{p}			
10		✓^{p}	✓^{p}			

Tab. 2. The performed computations.

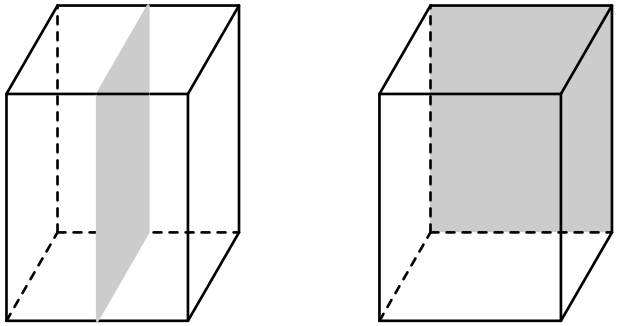

Fig. 3. The location of the selected atoms.

The immediate state of the selected atoms has been saved at every 50^{th} (sample A) or 25^{th} (sample B) simulation step in all the tests. The location of these selected atoms is shown in fig. 3. In this paper we present only some details due to the higher lucidity, see fig. 4. The state of the whole atomic system was saved when the simulations finished.

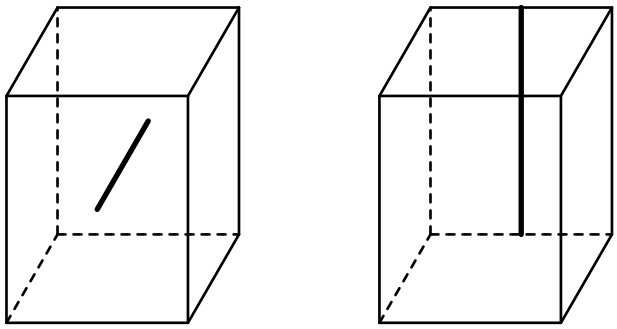

Fig. 4. The location of the atoms used in the following figures.

In the following figures we are concentrated only on the sample A and plane loading at the 2-nd, 4-th and 6-th stress level. Time development of the global kinetic and potential energies in the whole system is shown in the fig. 5, fig. 8 and fig. 11. In these figures, significant times from t_1 up to t_4 are marked by the vertical lines. At the time step t_1 the pressure wave front reaches the crack plane, at the time step t_2 the wave for stress level 4 passes the crack and the time steps t_3 and t_4 denote the moment, when the wave is detected closely before or after the reflection from the center of the back sample face (at the mentioned sampling rate, i.e. each 50^{th} step).

The courses of the atomic absolute velocity on the y axis are depicted in the fig. 6, fig. 9 and fig. 12 (see fig. 4-left) at the time steps t_1 and t_2 for the 2-nd, 4-th and 6-th stress level. The location of the crack is denoted in these figures by means of the gray line. It is visible from the fig. 6 that at the time step t_2 the wave did not pass through the crack. The local atomic interactions across crack faces do not occur before the waves scattered at the crack edges arrive to the back face of the crack. The fig. 9 shows that at the time step t_2 the wave already passed the crack and from the fig. 12 is obvious, that the pressure wave passed through the crack even before the time step t_2.

The situation at the atoms located on the perpendicular back face axis (see fig. 4-right) is illustrated in the fig. 7, fig. 10 and fig. 13, where the courses of atomic absolute velocity are depicted at the time steps t_3 and t_4 for the stress levels 2, 4 and 6.

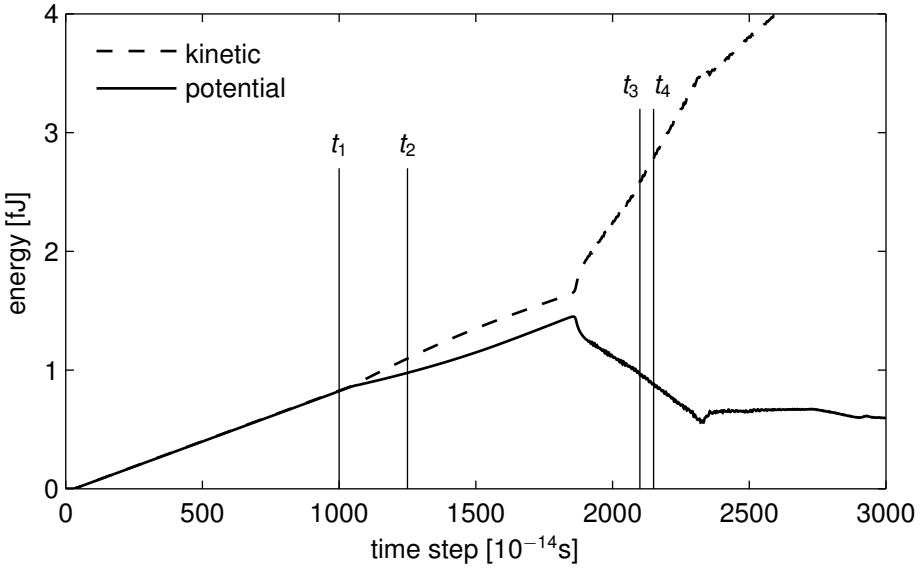

Fig. 5. The kinetic and potential energy of the whole system, loading level 2.

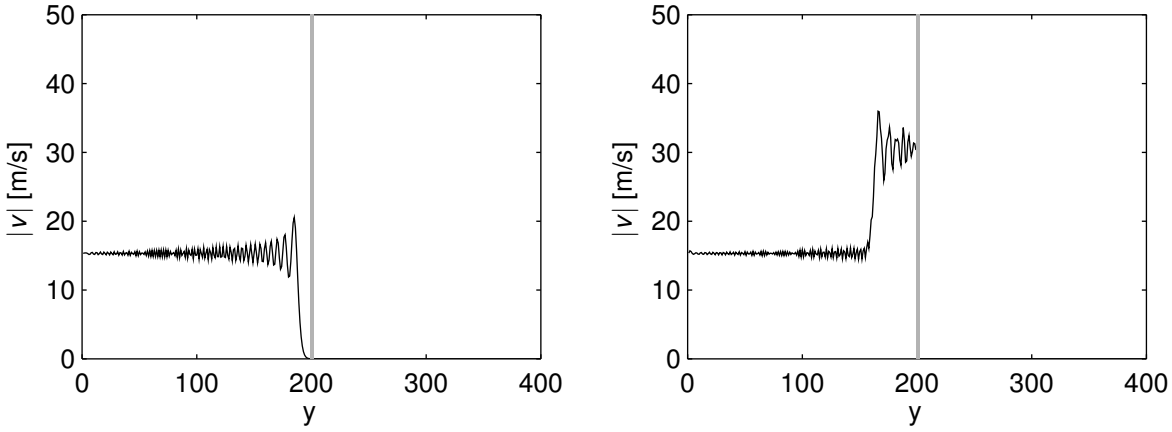

Fig. 6. Velocity magnitudes of the atoms on the y axis, loading level 2, time t_1 - left, t_2 - right.

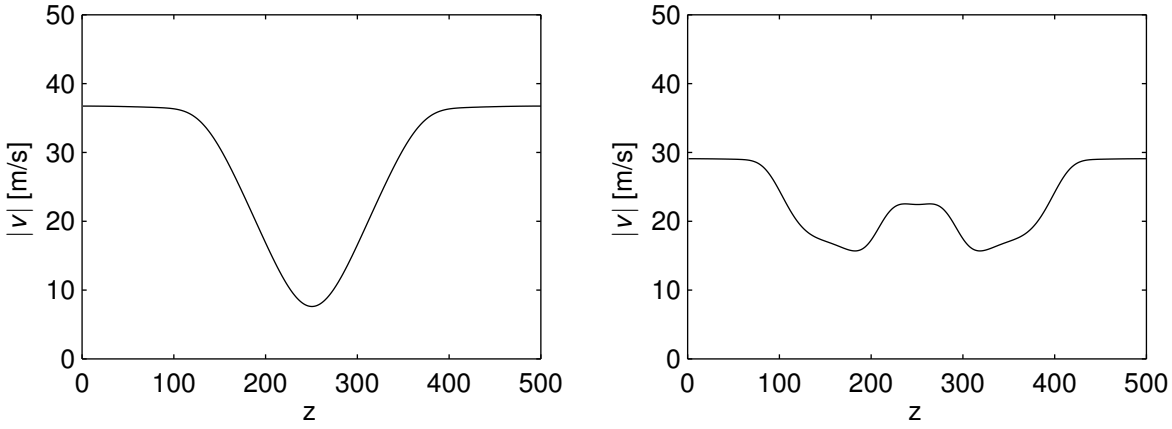

Fig. 7. Velocity magnitudes of the atoms in the z axis direction, loading level 2, time t_3 - left, t_4 - right.

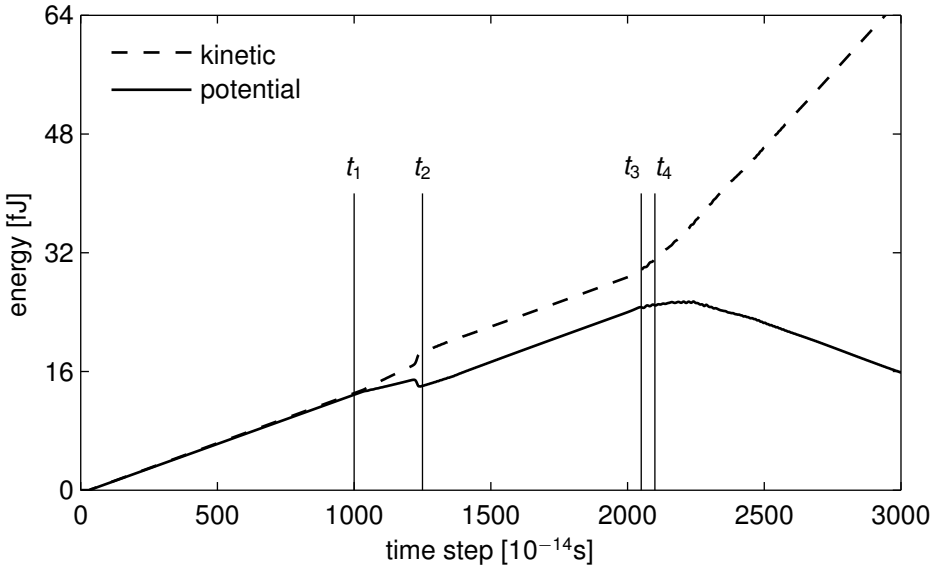

Fig. 8. The kinetic and potential energy of the whole system, loading level 4.

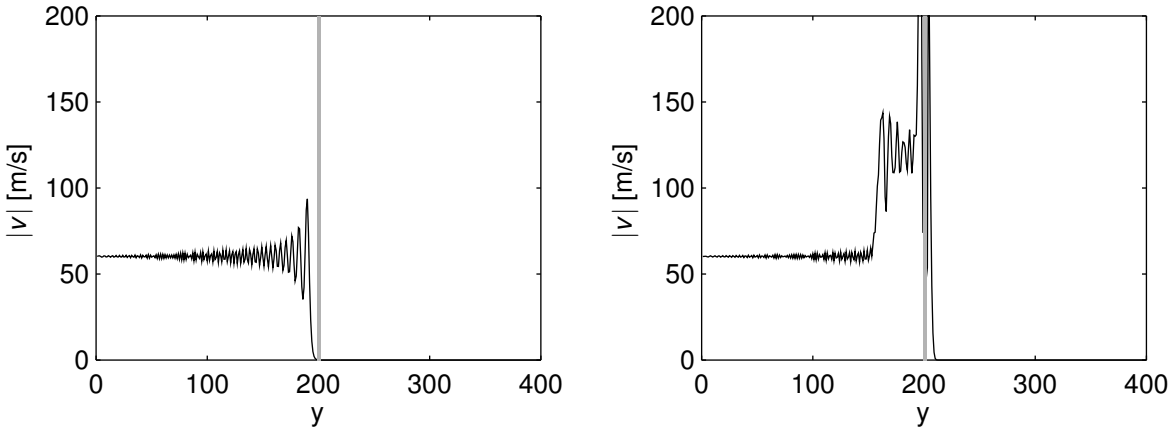

Fig. 9. Velocity magnitudes of the atoms on the y axis, loading level 4, time t_1 - left, t_2 - right.

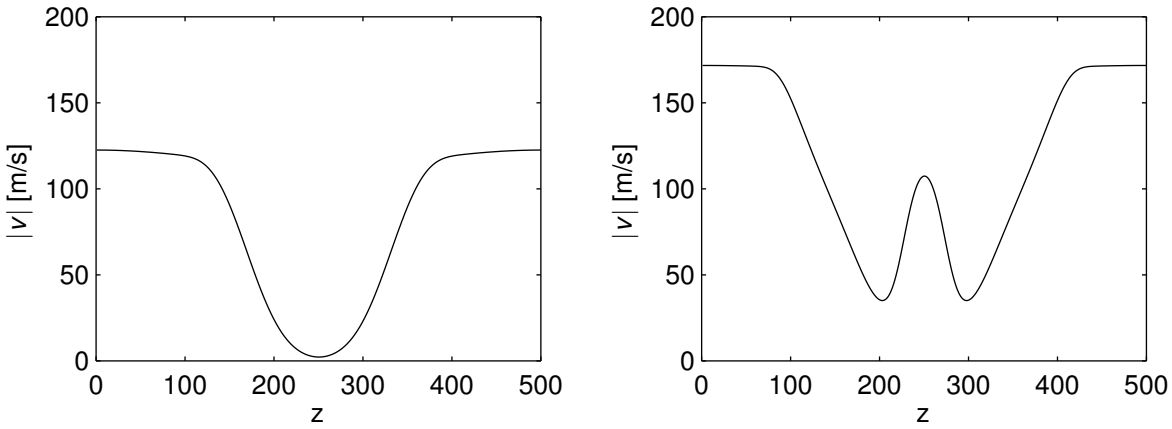

Fig. 10. Velocity magnitudes of the atoms in the z axis direction, loading level 4, time t_3 - left, t_4 - right.

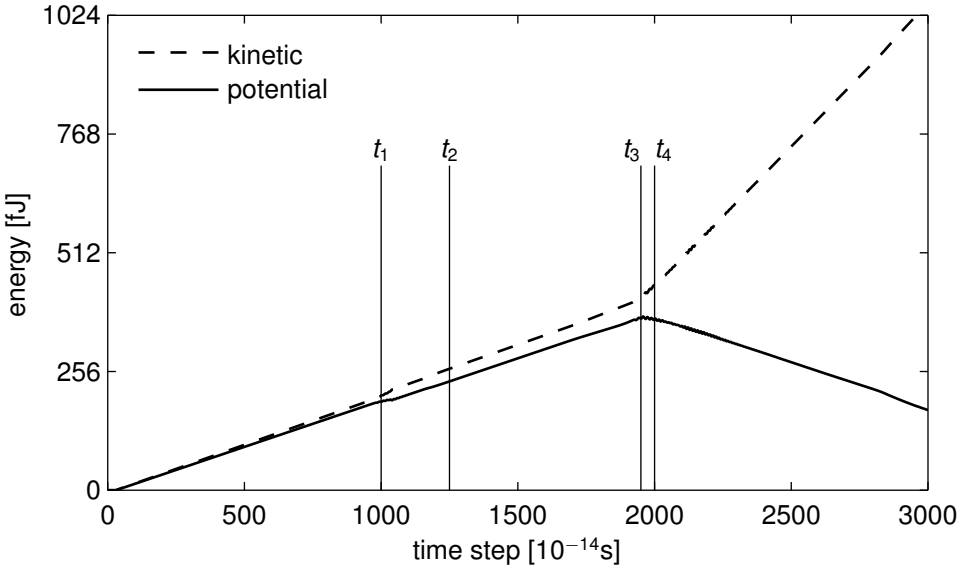

Fig. 11. The kinetic and potential energy of the whole system, loading level 6.

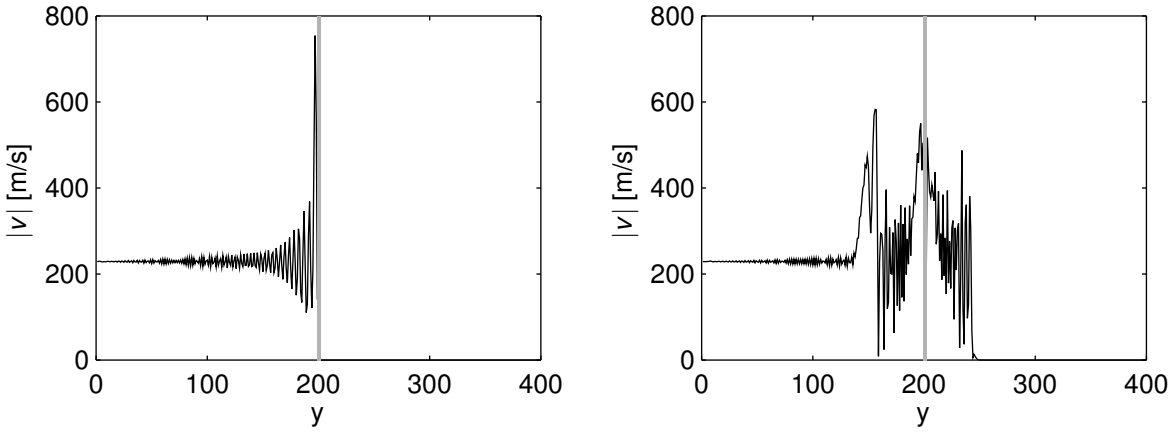

Fig. 12. Velocity magnitudes of the atoms on the y axis, loading level 6, time t_1 - left, t_2 - right.

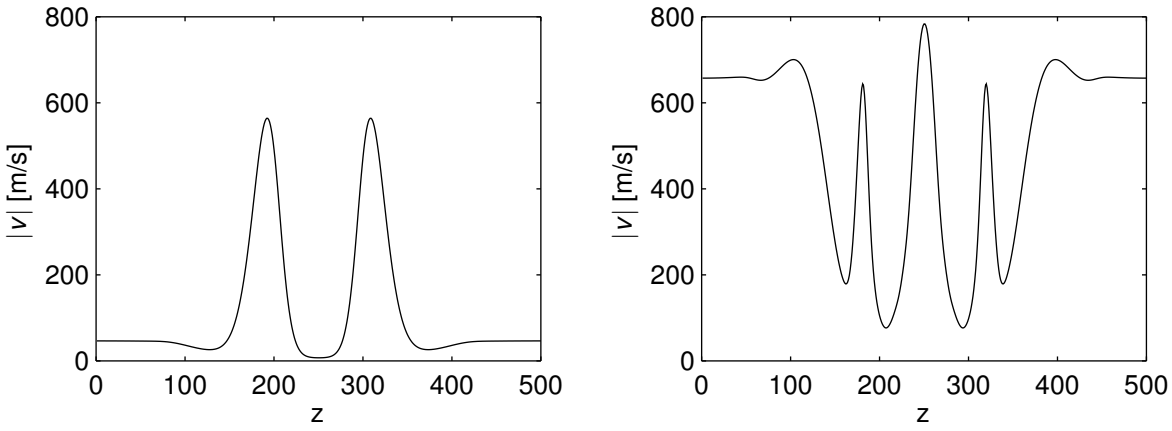

Fig. 13. Velocity magnitudes of the atoms in the z axis direction, loading level 6, time t_3 - left, t_4 - right.

4. Conclusion

The paper presents the first results of our research on propagation of pressure stress waves across a crack embedded in bcc iron crystals with the basic cubic orientation. A pre-existing Griffith (through) crack has been considered, where the local atomic interactions across the free crack faces do not exist initially. The simulations were based on molecular dynamic method and utilized an N-body potential of Finnis-Sinclair type for transition metals, [1], [2].

An important result is finding of the critical stress level, when the crack-grip occurs and consequently new local atomic interactions arise across the crack faces. It causes changes of the signal received on the opposite (initially unloaded) sample surface.

Our future research will be oriented on investigations of stress wave propagation after the critical interaction crack-pressure pulse and on a possible mapping of the internal cracks in materials via this non-linear phenomenon.

Acknowledgements

The work was supported by the Czech Science Foundation under the grant 101/07/0789 and the research project AV0Z20760514 of AS CR.

References

[1] G. J. Ackland et al., Computer simulation of point defect properties in dilute Fe-Cu alloy using a many-body interatomic potential, Phil. Mag. A, Vol. 75, 1997, s. 713-732.

[2] M. W. Finnis, J. E. Sinclair, A simple empirical N-body potential for transiton metals, Phil. Mag. A, Vol. 50, 1984, s. 45-55.

[3] P. Pacheco, Parallel Programming With MPI, Morgan Kaufmann, 1996.

[4] V. Pelikán, P. Hora, A. Machová, M. Landa, Ductile-Brittle Behavior of Microcracks in 3D, Materials Science Forum 482 (482) (2005) 131-135.

[5] V. Pelikán, P. Hora, A. Machová, A. Spielmannová, Brittle-ductile behavior in 3D iron crystals, Czechoslovak Journal of Physics 55 (10) (2005) 1245-1260.